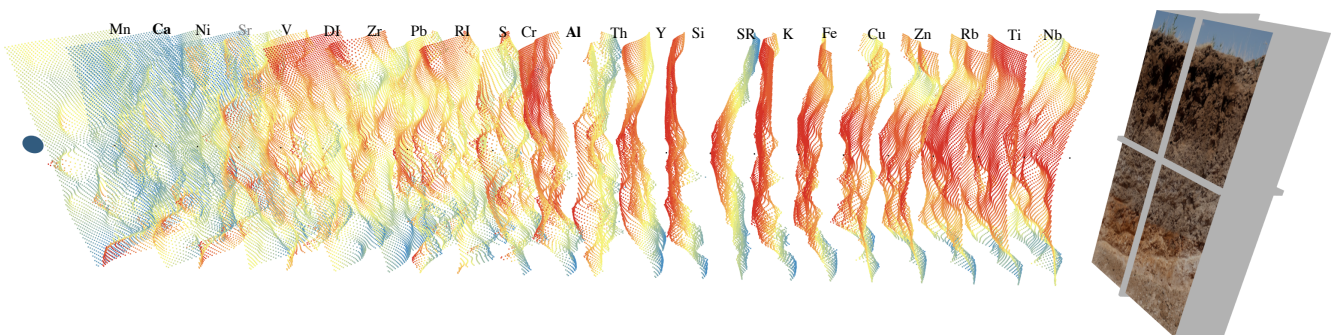


# SoilScanner: 3D Visualization for Soil Profiling using Portable X-ray Fluorescence

V. Pham<sup>1</sup>, D. Weindorf<sup>2</sup>, & T. Dang<sup>1</sup>

<sup>1</sup>Computer Science Department, <sup>2</sup>Plant and Soil Science, Texas Tech University, Lubbock, USA



**Figure 1:** 3D visualizations to describe the distributions of the detected chemical elements in a soil profile.

## Abstract

Soil scientists perform similar types of exploratory analysis repeatedly, such as generating the spatial distribution of chemical elements. The soil analysis process is time-consuming (may take days or weeks), labor-intensive (involving many people with different expertise for data collection, measurements, visual representation, and data analysis), and involving various tools (from traditional software, such as Microsoft Excel, to some complicated packages such as ArcGIS and MatLab). Inspired by medical scanning, this paper proposes a 3D visual solution, which can be generated via a web interface, allowing Soil scientists to perform on-the-field analysis. Our visualization prototype, named SoilScanner, supports a full range of interactive operations, such as ranking, filtering, brushing and linking, and detail on demand. We also demonstrated the usability of our SoilScanner visualizations on the soil profiles in West Texas, USA, collected via portable X-ray fluorescence spectrometers.

## 1. Introduction

Recent developments of field portable X-ray fluorescence spectrometers (pXRF) offer a rapid and cost-effective and non-invasive approach to quantify chemical elemental data [RT16]. The increasing adoption of these handheld devices leads to the availability of large pXRF chemical data to be analyzed. While the pXRF data availability increases rapidly, the analysis tasks encumber the further extensibility of this technique to an even broader scope. Specifically, due to the lack of expertise and the complexity of providing different visualization solutions for different individuals, manufacturers of pXRF devices currently offer limited data visualization solutions in their proximal sensors [PD19b]. These devices only provide some basic statistics (simple listing) incorporated into their device screens. These are mostly tabular format data displays or basic charts and usually do not scale well with the data sizes. There-

fore, analysts often need to create their own visualizations to suit their analysis purposes. They need to use traditional software (e.g., Microsoft Excel) or some complicated packages (e.g., ArcGIS and MatLab), or even programming languages (e.g., R or Python) to create custom visualizations for the analysis tasks.

On the other hand, visualizations offer several benefits for the exploration and analysis of complex environmental datasets and communication of the results to the public or stakeholders [RSK14]. Therefore, there is a requirement for interdisciplinary collaboration between the data visualization experts (to offer accurate visualizations) and the environmental domain experts (to improve the understanding and validate the accuracy of the analysis results). Therefore, in this project, we worked closely with two senior soil scientists to devise a solution to rapidly analyzing the pXRF available data.

## 2. Related Work

As using pXRF for quantifying the elemental contamination is rapid, cost-effective, and non-destructive, it has been applied in many different application domains. It is not possible to extensively survey all the works related to this domain. Thus, as the purpose of this paper, we are going to review the several recent works that utilize pXRF devices for collecting data and how the analysts utilize visualizations to analyze the data or to communicate the results to the public.

In the environmental assessments, Mukhopadhyay [MCB\*20] proposed a systematic approach to the analysis of soils using pXRF for the ecological evaluation. Also, Mukhopadhyay et al. [MCB\*20] assessed heavy metals and soil organic carbon using data collected from pXRF devices. In terms of agricultural impacts on the soil, Liu et al. [LLY\*20] used pXRF to assess the accumulation, sources, and potential ecological risk of potentially toxic elements in soil under vegetable production systems. In terms of the impacts of industrialization and population growth to the environments, Barbosa et al., [BPT\*20] assessed soil contamination in automobile scrap yards using pXRF. Also, Clinton et al., [CDS\*19] used the pXRF technology approach to the identification of trace metals and potential anthropogenic influences on the historic New York African Burial Ground population.

Soil quality is also an essential element in agriculture. Therefore, this technique is also applied to support agricultural activities. For instance, Alder et al. [APS\*20] used a pXRF device to measure 1,520 soil samples and used the measured data to assess copper (Cu), zinc (Zn), and cadmium (Cd) concentrations in agricultural soil. Similarly, [AFS\*20] used pXRF technology to evaluate soil fertility, and Silva et al. [SWP\*20] used pXRF data to predict soil texture variables (sand, silt, and clay). Besides a large number of researches in using pXRF devices in the analysis of soils, there are also works in analyzing lithostratigraphic units (e.g., shales and limestone). For example, Liu et al. [LSMT20] assessed the mechanical rock properties in tight shale, and Mastalerz et al. [MDAM19] stated that marine shale and limestone strata were clearly defined based on pXRF data.

In terms of utilizing the pXRF data, there are two main trends. The first is to show whether the elements of concerns (e.g., for soil fertility, assessments of heavy metals, rock properties) appear in the analyzing units (e.g., soil profiles and lithostratigraphic units) and how they are distributed (horizontally or vertically) in the units [LSMT20, MDAM19, MCB\*20, RWT20, LLY\*20, BPT\*20]. The second trend is to use pXRF approach as a low cost, effective, and non-destructive alternative to the slow, expensive conventional laboratory approaches to predictions of soil chemical properties [ASW\*20], soil texture [SWP\*20], tropical soil pH and sorption complex [dSTPF\*20], soil fertility [AFS\*20], and predictions of Cu, Zn, and Cd Concentrations in soil [APS\*20], to name but a few.

Regarding the utilization of visual representations, it is interesting that tables are commonly used to report findings. Specifically, tables appear in all the reviewed works. Also, the commonly used visualizations are bar charts (e.g., for showing the detected elemental concentration); line graphs, boxplots, and heatmaps (e.g.,

for showing spatial elemental distributions); scatterplots with regression line, and correlogram (e.g., for showing elemental correlations or the correlations between actual and predicted results); and ternary diagram (e.g., for explaining percentages of clay, sand, and silt). Also, most of these works use the combination of traditional software (e.g., Microsoft Excel) and geographic information software (e.g., ArcGIS and Graphpad Prism) [MCB\*20, CDS\*19] to analyze and generate their visualizations. Especially in many works, the analysts need to create their own visualizations using *R* programming language [AFS\*20, SWP\*20], Python [APS\*20], or JavaScript [DPNN20]. Our proposed approach allows non-professionals to generate the 3D chart of chemical concentrations without any knowledge of programming languages.

## 3. Motivations

As discussed in the previous section, the visualizations are limited, and most of these graphical representations are used to communicate the results to the public merely. They lack interactions to support further analysis and investigation. The use of software packages and especially programming languages to create different visualizations for different analysis purposes is a burden for the data analysts. On the other hand, many pieces of research in the literature suggest the beneficial uses of interactive visualizations for data analysis in various domains, from cybersecurity [PD18], abnormality detection [PD19a, PNL\*19], to efficient manufacturing [LPND19], to name but a few.

Furthermore, Pham, Dang [PD19b], and Sun et al., [SBD\*20] recently proposed an interactive visualization approach to analyzing soil profiles. In their works, data visualizers and soil scientists worked closely (as also suggested by Rink et al. [RSK14]) to discover and validate appropriate visualizations for soil profiling. These work are most related to ours in the literature, and we are not claiming to be superior to these work but rather to offer an alternative or extension to 3D profiling and visualizing soil chemicals via pXRF. We argue that this application is suitable for adopting 3D displays since the natures of soil profiling data is 3D [DRST14].

Our 3D approach to soil profiling is inspired by the medical scanning process, such as brain imaging [PWF\*16] and CT/Ultrasound scanning [GKL\*96], which allows doctors to continuously navigate different cuts of the brain/body. This feature is commonly supported in 3D-enabled software, such as ParaView [AGL05]. Similarly, in soil profile analysis, the soil scientists state that it is essential for them to navigate through vertical and horizontal slices of a soil profile and visually observe how the elemental distributions slowly change over the depths and space. The distributions in 3D help in quantitatively and perceptively differentiate the elemental spatial-distributions rather than merely perceptive cognition provided 2D approach, e.g., by using colors, as in 2D heatmaps, to display the values.

For instance, Figure 2 shows a typical soil profile analyzed using pXRF. From top to down, there are 13 soil horizons to be analyzed (named ‘A’ to ‘M’ correspondingly). Soil scientists also measure ten cells at every horizon (named as ‘1’ to ‘10’ from left to right, respectively) instead of one (as in the conventional approach to soil horizon analysis). This increment in the number of scanned cells

per horizon is to improve the accuracy, e.g., by averaging ten cells to get the elemental contamination at each horizon. In this case, they often need to scan from top to down to analyze the soil horizons. They also like to scan horizontally to see if the new approach (scanning ten cells instead of one) improves the analysis results.

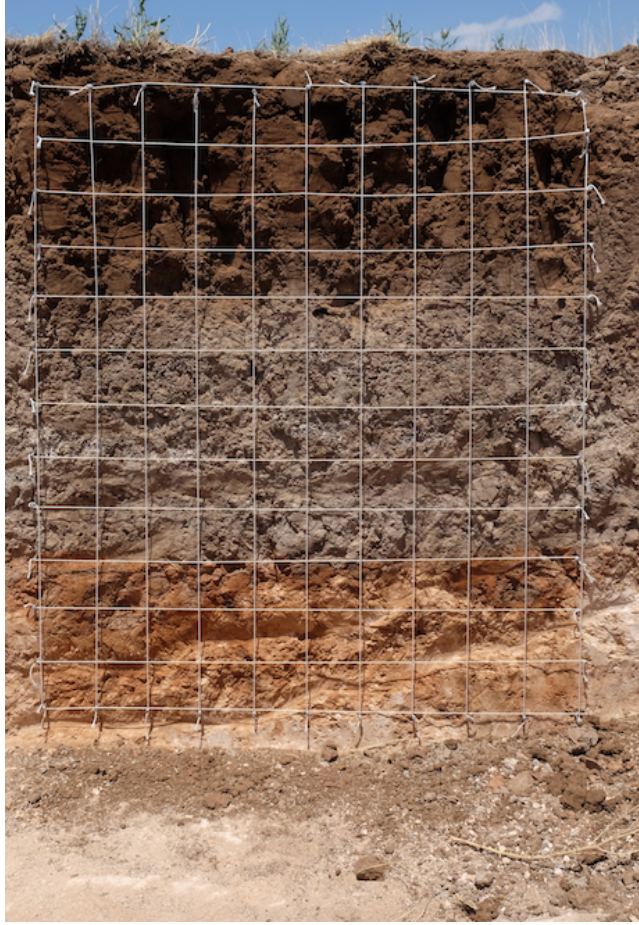


**Figure 2:** The grid layout of a soil profile: Vertically, there are 13 horizons (named as 'A' to 'M' from top to bottom correspondingly). Horizontally, there are vertical slices that the soil analysts need to measure (named as 'I' to 'X' from left to right, respectively). Each grid cell is of size  $10 \times 10$  cm.

#### 4. SoilScanner Stages

Figure 3 shows the main stages in our approach to soil horizon analysis using pXRF technology. First, the soil scientists collect the data at a geospatial location (this usually takes one day for the field trip) and then export the data in the data collection stage (Stage 1). The collected data is then cleaned and interpolated in the second stage (Stage 2). From there, the processed data is then imported, and detected elements are visualized (Stage 3). Finally, *SoilScanner* also provides interactive features to assist the analyst in examining the elemental distributions (Stage 4). Notice that stages 2, 3, and 4 take several days or even weeks since it may involve many people with different expertise. Our *SoilScanner* prototype cuts these

processed to a matter of a few seconds. This also means that human mistakes in data collection (for example, shooting the pXRF device to an undesirable position which does not reflect the real chemical concentrations) can be redone on the field, and therefore, we can save the researcher efforts to correct the mistakes. The rapid analysis also offers a means to do in-field analysis of pedological features using pXRF technology.

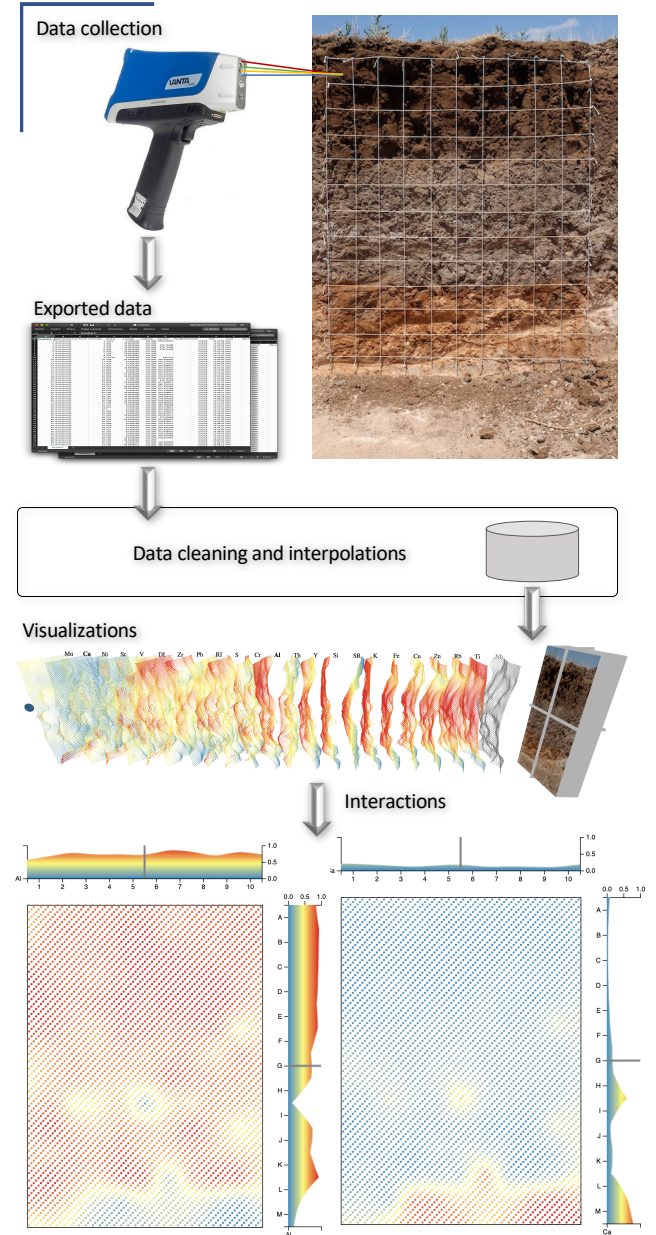


**Figure 3:** *SoilScanner* schematic overview. There are four main stages as (1) Data collection, (2) Data cleaning and interpolation, (3) Visualizations, and (4) Interactions.

#### 4.1. Data collection

In this stage, the soil scientists excavate and take a digital photograph of a soil profile (or pedon interchangeably in Pedology terminology). They then use strings to lay physical wireframes of size  $13 \times 10$  and each cell of size  $10 \times 10\text{cm}$  over the profile. The analysts then scan each cell of the wired grid with any number of proximal sensors (e.g., portable X-ray fluorescence, visible near-infrared spectroscopy) and then import the scanned (elemental) data into the visualization tool. As mentioned above, this is a time-consuming process (it may take a one-day field trip of three soil researchers to collect a single soil profile at a geographic location in West Texas).

#### 4.2. Data processing

The energy-disperse pXRF technology is good at detecting several chemical elements, but at the same time, it poorly determines several other chemical elements. The poor pXRF results for the latter are often due to their often low concentrations in the soil profile and also the high instrumental LODs (limit of detection) [GL18]. Therefore, after importing, the data is cleaned to remove the elements with LODs. Furthermore, outlying elemental information is statistically calculated and might be removed during the data processing process with the user's discretion [PD19a].

Furthermore, pXRF technology offers a means to do in-field analysis of pedological features, and opportunities to infer pedological processes with its ability to provide instant measurements that can be used to compute weathering indices and elemental ratios designed for these purposes [SCMM16]. Therefore, at this stage, we automatically compute and add *Ruxton Weathering Index* defined as  $\text{SiO}_2/\text{Al}_2\text{O}_3$  [Rux68]; *Desilication Index* defined as  $\text{SiO}_2/(\text{Al}_2\text{O}_3 + \text{Fe}_2\text{O}_3 + \text{TiO}_2)$  [SPS98], and *Elemental ratio of elements resistant to weathering, or Stable Index* for short defined as  $\text{Ti}/\text{Zr}$  [May92]. Figure 4 shows the 3D overview of these three indexes, which have been normalized and color-coded by the cell values (the soil scientists provide the color scale). There is a digital photo of the profile that helps to indicate the axes of these scatter-plots. However, in this figure, the digital photo is removed for space efficiency. Instead, we add x, y, and z axes for the horizons, vertical slices, and values of the pedological properties correspondingly. Also, the visualization generation is described in the next section.

Finally, it is not possible to scan every single point in a pedon. The scanned points are discretely distributed on every cell over the physical wireframes prepared. Thus, the elemental concentrations for each element are only available in  $13 \times 10$  discrete points, for each profile. However, the actual natural distributions of the elements are more or less continuous. Therefore, we interpolate the data using the Kriging algorithm [VB05]. Kriging is a smoothing method that soil scientists often use to interpolate the data spatially. Specifically, we use spherical Kriging model with  $\sigma^2 = 0$ ,  $\alpha = 100$  for the data interpolation process.

#### 4.3. Visualizations

After the processing stage, our system displays the data in several different ways. By default, all the detected elements plus the weathering indices and elemental ratios are displayed, as shown in Figure

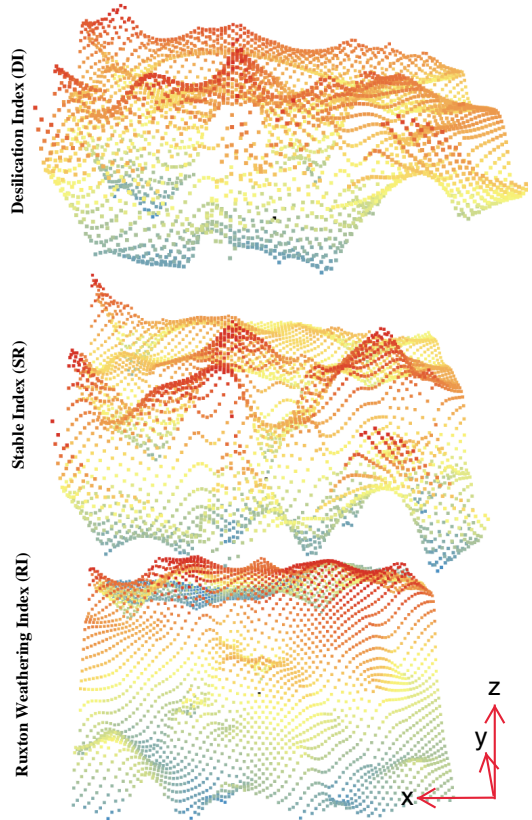


**Figure 4:** Our 3D scatter views of weathering indexes and elemental ratios for analyzing pedological features (computed directly from the chemical measurements collected via the pXRF device): Desilication Index (DI), Elemental ratio of elements resistant to weather or Stable Index (SR), and Ruxton Weathering Index (RI). The x, y, and z axes represent the profile horizons, profile vertical slices, and values of the pedological properties.

1. This visualization provides an overview of 3D distributions of the elements over the spatial space of the profile. Ranking and ordering the chemical elements enable grouping chemicals with similar concentration distributions together. This view also provides a digital photo of the pedon, taken at the data collection stage, in the background for better correlation of the elemental distributions and the underlying soil profile.

As discussed previously, the analysts often like to observe the elemental concentrations across the top-down horizons or left-right slices. We provide additional views that display elemental distributions at the specified horizons or vertical slices correspondingly. Figure 5 shows the concentrations for plant essential elements ('Ca', 'Cu', 'Fe', 'K', 'Mn', 'S', and 'Zn'). Specifically, the left panel shows the vertical distributions of these elements at vertical slice 5–6, and the right one depicts the horizontal distributions at the horizon 'G' for these elements. Different elements would have different value ranges and measurement units, and the analyst only likes to view their relative distributions (from 0 to the maximum value of an element over the profile as a whole). Therefore, the

distribution of an element is scaled from 0 to its maximum concentration value, of that element over all the cells in the profile, to [0, 1] range. The color scale goes from the blue for 0 and red for 1.

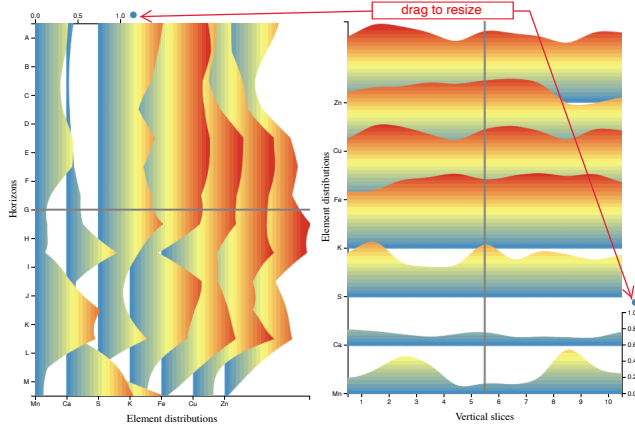


**Figure 5:** Concentrations for plant essential elements ('Ca', 'Cu', 'Fe', 'K', 'Mn', 'S', and 'Zn'): Vertical distribution at vertical slice 5-6 (left) and horizontal distribution at the horizon 'G' (right). The distribution is scaled from 0 to its maximum value over all the cells in the profile to [0, 1] range. The color scale, which is provided by the soil scientists, goes from the blue for 0 and red for 1. The order and resize options help to assure the front elements do not hide those in the back at the points of concerns (e.g., the cut point of the horizontal and vertical lines).

In this case, the line-graph is usually used by soil scientists to represent the elemental distributions. However, this solution suffers from cluttering issues when there is a large number of elements. The often-used solution to tackle this cluttering issue is to separate individual elements into different charts. However, this approach faces another obstacle which is the space limitations due to limited screen sizes. Therefore, we propose to use the elemental step-wise charts. In this approach, elements are not separated into different charts but rather shifted for a specified space. Space can be specified by the analysts, as described in the Interactions section. Once shifted, using line-graphs would lead to difficulties in recognizing the base of an individual element (since different elements would have different bases).

Therefore, instead of line-graphs, we use area-charts for these, because the solid fill in area-charts helps users to recognize the elemental bases [JME10]. The disadvantage of the filled area charts is that they may hide one another. We resolve this issue by providing options to order the elements so that the front elements always have lower values than the ones in the back at the points of concern. Thus, front elements are not hidden by the ones in the front, at least at the points of interest (based on ordering options). Furthermore, users also have an option to resize the chart size in such a way that it reduces overlapping between elements. The ordering and resize options are described more in Section 4.4. Via communication with the soil scientists, they stated that this is a more efficient approach. This situation also acts as a typical example of how the collaborative approach works [CGM\*17]. Specifically, the soil scientists

provide the requirements, and the data visualizers help in providing appropriate visualizations for their needs [CAS\*18].

Another frequent requirement from the soil scientists is to have details and compare two different elements to see their correlation in a soil profile. Therefore, *SoilScanner* provides two further details views at the bottom of the interface for this purpose, as shown at the bottom of Figure 3. In these two views, besides the 3D distributions of the selected elements over the whole profile, we also provide the area-charts to describe the elemental distributions over the currently selected horizon or vertical slice correspondingly.

#### 4.4. Interactions

*SoilScanner* is not just merely used for communicating the analyzed results to the public but also for analyzing the pXRF data. Therefore we provide menus and interactions to support the analysis tasks [AES05]. Specifically, Figure 6 shows the main menu of this application. *SoilScanner* provides options for the analyst to select a profile to be analyzed. There are three profiles provided by the soil scientists, and more profiles can be incorporated on demand. Also, whenever exploring the horizontal or vertical cut (indicated by the gray planes in the main views and the gray lines in the other views (i.e., area-charts), the analysts would like to have options to order the examining elements. The options include ordering the chemicals by their values (1) at the specific cut point (the intersection between the horizontal cut plane and vertical cut plane), (2) by the average of all the values of the element across the specified horizontal line, or (3) similar to the second option but for the vertical line. For all these cases, the order is always ascending, as we are using step-wise area-charts, the elements at the back should always have higher heights, so they are not hidden by the ones in the front.

The main views and the two elemental details views (as shown in Figure 1 and Figure 5, respectively) that are used to compare the selected elements are both in 3D. Therefore, users can use orbit controls, which provide zooming, rotating, and panning options, to view the elemental distributions at different distances/angles. To quickly get back to the default views, users can use the options at the bottom of Figure 6 to reset the main views, the details views, or all the views correspondingly.

Often, pXRF devices can detect about 20 to 23 chemical elements of concerns. Some others are not detectable due to their concentrations are smaller than the LODs of the devices. Displaying all of the detected elements to the soil scientists, as displayed in our *SoilScanner* default interface, would be overwhelmed. Therefore, at the top of the program, we also list these elements with corresponding check-boxes. Users can select/deselect individual elements, in case needed, using the provided check-boxes.

Furthermore, soil scientists frequently analyze related elements of defined packages. A package is a set of elements related to a specific analysis need. For instance, Figure 7 shows two examples of packages defined by soil scientists. The first one (on the left) is the package for 'plant essential elements'. These elements are of concern when analyzing the fertility of the soil profile for agricultural purposes. The second one (on the right) are the heavy metals (those inside the parentheses are ones that might not be detectable

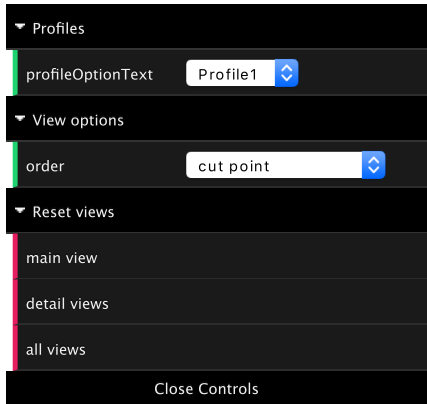


**Figure 6:** SoilScanner provides options to select different profiles to analyze; to order the elements in the main views and the horizontal/vertical distributions views; and to reset the views to the default arrangements (if the views are changed, e.g., using orbit controls).

by pXRF devices). These heavy metals are essential when scientists analyze environmental issues. Other packages are individual elements related to the weathering indices or elemental ratios (described in Section 4.2) or another higher level package that includes all these indices and ratios. Using the check-boxes for packages, users can conveniently toggle the whole group of elements within each package.



**Figure 7:** Two examples for packages of elements: Plant essential elements (left) and heavy metals (right). They can be selected/deselected individually or by their groups. Those elements inside the parentheses for heavy metals mean they might not be detectable by the pXRF device.

For the ease of use and convenience for the users, whenever possible, we provide direct interactions to the visualizations [PSCO09]. For instance, there are two planes in the cube with the background image (at the far right of Figure 1). These planes represent the horizontal and vertical cut planes at the soil profile accordingly. The soil analyst can drag these two planes over the pedon to scan the elemental distributions (as shown in Figure 8). While scanning, all the elements are ordered in the views (as in Figure 1 and Figure 5) accordingly by the selected ordering option. Furthermore, on the details views, there are also gray lines indicating the current horizontal/vertical scanning positions.

Also, the displays for the elements might be dense or sparse, depending on the number of chemicals to be analyzed (which can be adjusted by the users). Therefore, we provide options to resize the space between elements. Specifically, at the far left of the main view, as shown in Figure 1, the user drags the blue sphere to compress/expand the distances between elements in that view. Similarly, users can use the two blue circles, indicated by the red call-out in Figure 8, to resize the height of the area-charts for the elemental

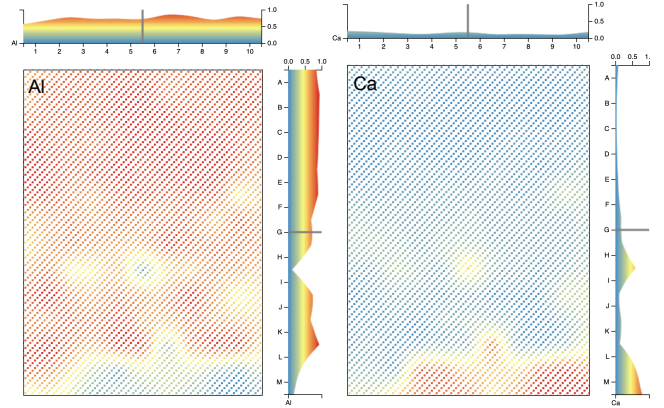


**Figure 8:** Details views for two individual elements to be compared ('Al' on the left and 'Ca' on the right). There are also area charts above and on the right of each view to show the elemental distribution at the specified horizon or vertical slice correspondingly.

distributions. Once resized, the step size (distance between the base of every two elements) is also updated accordingly to distribute the area-charts evenly in the views.

## 5. Implementation

SoilScanner is implemented as web-based application using JavaScript D3.js [BOH11] library and JavaScript 3D library called three.js [Dan12]. The source codes and the web application of our visualization are available on our Github project at <http://idatavisualizationlab.github.io/Soil/soil3d.html>.

## 6. Evaluations

While developing this visualization solution, we followed the approach proposed in [RSK14] to work closely with two soil scientists: One post-doc researcher and a senior Professor with more than ten years of experience in analyzing soil horizons and soil profiling with pXRF devices. While the soil scientists help to understand the data and provide domain-specific requirements, the data visualizers assist in specifying appropriate visualizations for these requirements. Especially, we do not just merely use the visualizations to communicate the findings but also use SoilScanner to analyze the data by providing interactive options for the visualizations.

The process of eliciting the requirements, developing, and validating the results happened iteratively during the development of this project. We received positive feedback from the soil scientists, and they also indicated that a tangential adaptation of the aforementioned approach could be applied to cores extracted from the earth. The cores would be easier to extract compared to having to excavate the whole large soil pedons, thus leading to a larger amount of data. Also, we can use 3D visualizations to analyze and intuitively visualize different agricultural/environmental issues in more significant geographic regions. Furthermore, they would also like us to incorporate machine learning elements in our solution (1) to suggest personalized and appropriate graphs to the users for the

underlying data, depending on users profiles and interactions, and (2) to predict soil or other chemical properties (e.g., soil fertility, soil texture, lithostratigraphic properties) from pXRF data instead of having to go through slow and costly laboratory procedures to quantify these properties.

## 7. Conclusion and Future work

In this work, we worked closely with soil scientists to elicit common exploratory tasks in analyzing soil profiles and provide appropriate data visualizations and analysis solutions in a web-based application called *SoilScanner*. This solution does not just help to communicate the soil profile analysis results to the public but also helps in analyzing tasks by providing a set of built-in calculations and interactions. Furthermore, a tangential adaptation of this approach can be applied to cores extracted from the earth for the analysis in larger geographic areas. Also, in the future, we will add the features so that the tool can use machine learning techniques to recommend graphs that are of interest to individual users based on their context. The context includes user profile, abstraction level, statistical quantification, and visual types. Finally, machine learning methods can also be incorporated in this solution to provide in-field information such as soil or lithostratigraphic features from the collected pXRF data instead of having to go through lengthy and expensive laboratory works.

## References

- [AES05] AMAR R., EAGAN J., STASKO J.: Low-level components of analytic activity in information visualization. In *Proc. of the IEEE Symposium on Information Visualization* (2005), pp. 15–24. [5](#)
- [AFS\*20] ANDRADE R., FARIA W. M., SILVA S. H. G., CHAKRABORTY S., WEINDORF D. C., MESQUITA L. F., GUILHERME L. R. G., CURI N.: Prediction of soil fertility via portable x-ray fluorescence (pxrf) spectrometry and soil texture in the brazilian coastal plains. *Geoderma* 357 (2020), 113960. [2](#)
- [AGL05] AHNRENS J., GEVECI B., LAW C.: Paraview: An end-user tool for large data visualization. *The visualization handbook* 717 (2005). [2](#)
- [APS\*20] ADLER K., PIKKI K., SÖDERSTRÖM M., ERIKSSON J., ALSHIBABI O.: Predictions of cu, zn, and cd concentrations in soil using portable x-ray fluorescence measurements. *Sensors* 20, 2 (2020), 474. [2](#)
- [ASW\*20] ANDRADE R., SILVA S. H. G., WEINDORF D. C., CHAKRABORTY S., FARIA W. M., MESQUITA L. F., GUILHERME L. R. G., CURI N.: Assessing models for prediction of some soil chemical properties from portable x-ray fluorescence (pxrf) spectrometry data in brazilian coastal plains. *Geoderma* 357 (2020), 113957. [2](#)
- [BOH11] BOSTOCK M., OGIEVETSKY V., HEER J.: D<sup>3</sup> data-driven documents. *IEEE transactions on visualization and computer graphics* 17, 12 (2011), 2301–2309. [6](#)
- [BPT\*20] BARBOSA J. Z., POGGERE G. C., TEIXEIRA W. W. R., MOTTA A. C. V., PRIOR S. A., CURI N.: Assessing soil contamination in automobile scrap yards by portable x-ray fluorescence spectrometry and magnetic susceptibility. *Environmental Monitoring and Assessment* 192, 1 (2020), 46. [2](#)
- [CAS\*18] COLLINS C., ANDRIENKO N., SCHRECK T., YANG J., CHOO J., ENGELKE U., JENA A., DWYER T.: Guidance in the human–machine analytics process. *Visual Informatics* 2, 3 (2018), 166 – 180. [5](#)
- [CDS\*19] CLINTON C. K., DUNCAN C. M., SHAW R. K., JACKSON L., JACKSON F. L.: Identification of trace metals and potential anthropogenic influences on the historic new york african burial ground population: A pxrf technology approach. *Scientific Reports* 9, 1 (2019), 1–10. [2](#)
- [CGM\*17] CENEDA D., GSCHWANDTNER T., MAY T., MIKSCH S., SCHULZ H., STREIT M., TOMINSKI C.: Characterizing guidance in visual analytics. *IEEE Transactions on Visualization and Computer Graphics* 23, 1 (Jan 2017), 111–120. [5](#)
- [Dan12] DANCHILLA B.: *Three.js Framework*. Apress, Berkeley, CA, 2012, pp. 173–203. [6](#)
- [DPNN20] DANG T., PHAM V., NGUYEN H. N., NGUYEN N. V.: Agasedviz: visualizing groundwater availability of ogallala aquifer, usa. *Environmental Earth Sciences* 79, 5 (2020), 1–12. [2](#)
- [DRST14] DUBEL S., ROHLIG M., SCHUMANN H., TRAPP M.: 2d and 3d presentation of spatial data: A systematic review. In *2014 IEEE VIS International Workshop on 3DVis (3DVis)* (Los Alamitos, CA, USA, nov 2014), IEEE Computer Society, pp. 11–18. [2](#)
- [dSTPF\*20] DOS SANTOS TEIXEIRA A. F., PELEGRINO M. H. P., FARIA W. M., SILVA S. H. G., GONÇALVES M. G. M., JÚNIOR F. W. A., GOMIDE L. R., JÚNIOR A. L. P., DE SOUZA I. A., CHAKRABORTY S., ET AL.: Tropical soil ph and sorption complex prediction via portable x-ray fluorescence spectrometry. *Geoderma* 361 (2020), 114132. [2](#)
- [GKL\*96] GENNART B., KRUMMENACHER B., LANDRON L., HERSCHE R. D., SAUGY B., HADORN J.-C., MÜLLER D.: The giga view multiprocessor multidisk image server. *Scientific Programming* 5 (03 1996), 3–13. [2](#)
- [GL18] GALLHOFER D., LOTTERMOSER B. G.: The influence of spectral interferences on critical element determination with portable x-ray fluorescence (pxrf). *Minerals* 8, 8 (2018), 320. [4](#)
- [JME10] JAVED W., McDONNEL B., ELMQVIST N.: Graphical perception of multiple time series. *IEEE Transactions on Visualization and Computer Graphics* 16, 6 (Nov 2010), 927–934. [5](#)
- [LLY\*20] LIU G., LIU B., YANG L., HU W., QU M., LU F., HUANG B.: Using pxrf to assess the accumulation, sources, and potential ecological risk of potentially toxic elements in soil under two greenhouse vegetable production systems in north china. *Environmental Science and Pollution Research* (2020), 1–11. [2](#)
- [LPND19] LE D. D., PHAM V., NGUYEN H. N., DANG T.: Visualization and explainable machine learning for efficient manufacturing and system operations. *Smart and Sustainable Manufacturing Systems* (2019). [2](#)
- [LSMT20] LIU B., SCHIEBER J., MASTALERZ M., TENG J.: Variability of rock mechanical properties in the sequence stratigraphic context of the upper devonian new albany shale, illinois basin. *Marine and Petroleum Geology* 112 (2020), 104068. [2](#)
- [May92] MAYNARD J.: Chemistry of modern soils as a guide to interpreting precambrian paleosols. *The Journal of Geology* 100, 3 (1992), 279–289. [4](#)
- [MCB\*20] MUKHOPADHYAY S., CHAKRABORTY S., BHADORIA P., LI B., WEINDORF D. C.: Assessment of heavy metal and soil organic carbon by portable x-ray fluorescence spectrometry and nixpro™ sensor in landfill soils of india. *Geoderma Regional* 20 (2020), e00249. [2](#)
- [MDAM19] MASTALERZ M., DROBNAIK A., AMES P., MC LAUGHLIN P. I.: Application of pxrf elemental analysis and organic petrography in correlation of pennsylvanian strata: An example from the indiana part of the illinois basin, usa. *International Journal of Coal Geology* 216 (2019), 103342. [2](#)
- [PD18] PHAM V., DANG T.: Cvexplorer: Multidimensional visualization for common vulnerabilities and exposures. In *2018 IEEE International Conference on Big Data (Big Data)* (Seattle, WA, USA, USA, Dec 2018), IEEE, pp. 1296–1301. [2](#)
- [PD19a] PHAM V., DANG T.: Outliagnostics: Visualizing temporal discrepancy in outlying signatures of data entries, 2019. [2, 4](#)

- [PD19b] PHAM V., DANG T.: SOAViz: Visualization for Portable X-ray Fluorescence Soil Profiles. In *Workshop on Visualisation in Environmental Sciences (EnvirVis)* (Porto, Portugal, 2019), Bujack R., Feige K., Rink K., Zeckzer D., (Eds.), The Eurographics Association. 1, 2
- [PNL\*19] PHAM V., NGUYEN N., LI J., HASS J., CHEN Y., DANG T.: Mtsad: Multivariate time series abnormality detection and visualization. In *2019 IEEE International Conference on Big Data (Big Data)* (2019), IEEE, pp. 3267–3276. 2
- [PSCO09] PIKE W. A., STASKO J., CHANG R., O’CONNELL T. A.: The science of interaction. *Information Visualization* 8, 4 (2009), 263–274. 6
- [PWF\*16] PANTA S. R., WANG R., FRIES J., KALYANAM R., SPEER N., BANICH M., KIEHL K., KING M., MILHAM M., WAGER T. D., TURNER J. A., PLIS S. M., CALHOUN V. D.: A tool for interactive data visualization: Application to over 10,000 brain imaging and phantom mri data sets. *Frontiers in Neuroinformatics* 10 (2016), 9. 2
- [RSK14] RINK K., SCHEUERMANN G., KOLDITZ O.: Visualisation in environmental sciences, 2014. 1, 2, 6
- [RT16] ROUILLO M., TAYLOR M. P.: Can field portable x-ray fluorescence (pxrf) produce high quality data for application in environmental contamination research? *Environmental Pollution* 214 (2016), 255–264. 1
- [Rux68] RUXTON B. P.: Measures of the degree of chemical weathering of rocks. *The Journal of Geology* 76, 5 (1968), 518–527. 4
- [RWT20] RAVANSARI R., WILSON S. C., TIGHE M.: Portable x-ray fluorescence for environmental assessment of soils: Not just a point and shoot method. *Environment international* 134 (2020), 105250. 2
- [SBD\*20] SUN F., BAKR N., DANG T., PHAM V., WEINDORF D. C., JIANG Z., Li H., WANG Q.-B.: Enhanced soil profile visualization using portable X-ray fluorescence (PXRF) spectrometry. *Geoderma* (2020). 2
- [SCMM16] STOCKMANN U., CATTLE S., MINASNY B., McBRATNEY A. B.: Utilizing portable x-ray fluorescence spectrometry for in-field investigation of pedogenesis. *Catena* 139 (2016), 220–231. 4
- [SPS98] SINGH L. P., PARKASH B., SINGHVI A.: Evolution of the lower gangetic plain landforms and soils in west bengal, india. *Catena* 33, 2 (1998), 75–104. 4
- [SWP\*20] SILVA S. H. G., WEINDORF D. C., PINTO L. C., FARIA W. M., JUNIOR F. W. A., GOMIDE L. R., DE MELLO J. M., DE PÁDUA JUNIOR A. L., DE SOUZA I. A., DOS SANTOS TEIXEIRA A. F., ET AL.: Soil texture prediction in tropical soils: A portable x-ray fluorescence spectrometry approach. *Geoderma* 362 (2020), 114136. 2
- [VB05] VAN BEERS W.: Kriging metamodeling in discrete-event simulation: an overview. In *Proceedings of the 37th conference on Winter simulation* (2005), Winter Simulation Conference, pp. 202–208. 4